International Journal of Nanomedicine

Dovepress
open access to scientific and medical research

Open Access Full Text Article

ORIGINAL RESEARCH

Berberine-Loaded Nanostructured Lipid Carriers Enhance the Treatment of Ulcerative Colitis

This article was published in the following Dove Press journal:
International Journal of Nanomedicine

Jianping Deng[1,2]
Zicong Wu[1,2]
Zhenling Zhao[2,3]
Chaoxi Wu[2,3]
Min Yuan[1]
Zhengquan Su[1]
Yifei Wang[2,3]
Zhiping Wang[1,2]

[1]Guangdong Provincial Engineering Center of Topical Precise Drug Delivery System, Department of Pharmaceutics, Guangdong Engineering Research Center of Natural Products and New Drugs, Guangdong Provincial University Engineering Technology Research Center of Natural Products and Drugs, Guangdong Pharmaceutical University, Guangzhou 510000, People's Republic of China; [2]Guangzhou (Jinan) Biomedical Research and Development Center, Guangzhou 510000, People's Republic of China; [3]College of Life Science and Technology, Jinan University, Guangzhou 510000, People's Republic of China

Purpose: Berberine (BBR), a major ingredient extracted from *Coptis chinensis*, is a natural drug with limited oral bioavailability. We developed nanostructured lipid carriers (NLCs) as a delivery system for enhanced anti-inflammatory activity of BBR against ulcerative colitis (UC).

Methods: BBR-loaded nanostructured lipid carriers (BBR-NLCs) prepared via high-pressure homogenization were evaluated for particle size, zeta potential, drug entrapment efficiency, drug loading, drug release, toxicity, and cellular uptake. The anti-UC activities of free and encapsulated BBR were evaluated in a DSS-induced acute model of UC in mice.

Results: Spherical BBR-NLCs were prepared with a particle size of 63.96± 0.31 nm, a zeta potential of +3.16 ± 0.05 mV, an entrapment efficiency of 101.97±6.34%, and a drug loading of 6.00±0.09%. BBR-NLCs showed excellent biocompatibility in vivo. Cellular uptake experiments showed that BBR-NLCs improved uptake of BBR by RAW 264.7 cells and Caco-2 cells. Oral administration of BBR-NLCs significantly alleviated colitis symptoms (DAI, colon length, spleen swelling, MPO activity) through inhibition of NF-κB nuclear translocation, decreased expression of pro-inflammatory cytokines (IL-1β, IL-6, MMP-9, CX3CR1, COX-2, TERT), and increased expression of the tight junction protein ZO-1.

Conclusion: BBR-loaded NLCs improved colitis symptoms, which suggested that this may be a novel formulation for treatment of UC.

Keywords: berberine, nanostructured lipid carriers, anti-inflammatory, ulcerative colitis

Introduction

Ulcerative colitis (UC) is a relapsing intestinal inflammatory disease with unknown etiology characterized by continuous diffuse inflammation and damage to the intestinal mucosal barrier.[1,2] The typical age of onset is between 20 and 39 years.[3] The incidence of UC is increasing annually worldwide, especially in Europe.[4] Drugs used to treat UC, including immunosuppressants, biological agents, glucocorticoids, amino acids, and salicylic acid, have side effects, and patient compliance is poor due to the chronic nature of the disease.[5] Recent studies have shown that natural products may be promising alternative agents for treatment of colitis.[6–9] However, many natural drugs are poorly soluble, which limits absorption, and results in low bioavailability.[10] New formulations of natural products to improve absorption and bioavailability have received increasing interest.[11,12]

Berberine (BBR) is the principal isoquinoline alkaloidal constituent of the stems and roots of various berberis species such as *B. aristata, B. petiolaris* and *B. vulgaris*.[13] Studies have shown that BBR exerts anti-inflammatory,[14] anti-oxidative,[15] and anti-hyperglycemic effects, and has anti-bacterial properties

Correspondence: Yifei Wang; Zhiping Wang
Email twang-yf@163.com; wzping-jshb@gdpu.edu.cn

submit your manuscript | www.dovepress.com
DovePress
http://doi.org/10.2147/IJN.S247406

associated with improvement of diarrhea and other gastrointestinal infections.[16] However, BBR suffers from poor aqueous solubility, poor absorption by the gastrointestinal tract, and low bioavailability (about 5%). Therefore, BBR must be administered at very high concentrations to achieve efficacy, which results in increased risk of adverse drug reactions.[17]

Recent studies have focused on nanocrystallization of natural products.[18–20] Lipid-based nanoparticles, which include solid lipid nanoparticles (SLN) and nanostructured lipid carriers (NLCs), are excellent drug delivery systems for lipophilic pharmaceuticals.[21–23] Nanostructured lipid carriers share the benefits of SLNs, such as stability, biocompatibility, biodegradability, and scalability, but allow for higher drug-loading capacity than SLNs due to greater structural disorder and reduced leakage of encapsulated drugs during storage.[24]

In this study, we developed BBR-loaded NLCs (BBR-NLCs) using high-pressure homogenization, and tested the physical features of this formulation. We then evaluated biocompatibility and drug uptake in vivo and in vitro. Finally, we evaluated the efficacy of BBR-NLCs for treatment of dextran sulfate sodium (DSS)-induced colitis in mice and explored the anti-inflammatory mechanisms of BBR-NLCs using Raw264.7 cells.

Materials and Methods

Preparation of NLCs Containing BBR

BBR-NLCs were prepared using high-pressure homogenization. Briefly, 2.5% glyceryl behenate (Compritol 888 ATO, GATTEFOSSE SAS, France) and 2.0% olive oil (Aladdin, China) were mixed and heated to about 75 °C (above the melting point). Then, 1.0% BBR powder (95%, Yuanye Bio-Technology, Shanghai, China), 2.0% cremophor EL (Kolliphor EL, BASF Corp., Germany), and 2.5% d-α-tocopheryl polyethylene glycol 1000 succinate (TPGS, BASF Corp., Germany) were dissolved in distilled water and heated to about 75 °C. The aqueous phase was dispersed into melted lipid solution, then homogenized at 5,000 rpm for 15 minutes (IKA T18 basic ULTRA-TURRAX®, Germany). This pre-mix was passed through a high-pressure homogenizer (APV-2000, Denmark) for 10 cycles at 500 bar and 20 cycles at 1,500 bar.

Characterization of BBR-NLCs

Diluted BBR-NLC (1:100) was placed on mica plates. After 10 min, the plates were analyzed using atomic force microscopy (AFM), and data were collected at room temperature using a Multimode-Nanoscope V (Veeco, USA) operated in ScanAsyst mode with an etched silicon probe (RTesp-Bruker; cantilever resonance frequency: 150 kHz, Force constant: 5 N/m, scan rates: 1 Hz).[25]

The BBR-NLCs were diluted 100-fold, then analyzed using a Malvern Zetasizer Nano-ZS (Malvern, Worcestershire, UK) to determine average particle size, polydispersity index (PDI), and zeta potential. Each analysis was performed in triplicate.

Nanostructured lipid carriers containing BBR were diluted 100-fold, and free drug was removed using a dialysis tube.[26] Then, BBR was extracted from the NLCs by addition of methanol. The drug content was determined at 263 nm using UV–Vis spectrophotometer (Shimadzu Seisakusho, Ltd., Kyoto, Japan). The experiment was performed in triplicate. The entrapment efficiency (EE) and drug loading (DL) were calculated using the following equation:

$$\mathrm{EE}(\%) = \frac{\text{drug released from the NLCs}}{\text{drug input}} \times 100\%$$

$$\mathrm{DL}(\%) = \frac{\text{drug released from the NLCs}}{\text{all materials input}} \times 100\%$$

All procedures were executed based on methods described by Zhang.[27] Briefly, adding 0.5 g of BBR or BBR-NLCs to 500 mL of simulated gastric juice (pH = 1.2) and stimulated intestinal juice (pH = 7.5) at 36 ± 0.5°C while stirring constantly at 50 rpm. At pre-determined time intervals, suitable aliquots were withdrawn, filtered with 0.45 μm pore size syringe filters, and assayed by above HPLC method. The withdrawn samples were replaced by equal volumes of fresh dissolution medium maintained at the same temperature.

Cell Lines and Cultures

The RAW264.7 and Caco-2 cells were purchased from the Cell Culture Center of the Shanghai Institutes for Biological Sciences of the Chinese Academy of Sciences (Shanghai, China) and maintained in Dulbecco's Modified Eagle Medium (DMEM) (Gibco BRL, Life Technologies, USA) supplemented with 10% fetal bovine serum (Invitrogen, New York, USA), 1% nonessential amino acids (Gibco BRL, Life Technologies, USA) (only Caco-2 cells), and 100 U/mL of penicillin and 100 μg/mL of streptomycin, and were cultured at 37°C in a 5% CO_2 atmosphere.

Biocompatibility Assays

Biocompatibility of BBR-NLCs was evaluated in vivo using a mouse model of colitis (Figure 1A). Toxicity was evaluated in vivo for 4 days following oral administration of blank NLCs, free BBR, and BBR-NLCs (20 mg/Kg). Six mice were assessed in each group. Major organs (heart, liver, spleen, lung, and kidney) were collected for analysis. Pathological changes were observed using a microscope.

Cellular Uptake Study

Caco-2 cells and RAW 264.7 cells (20×10^5 cells/well) were seeded in 6-well plates. On the second day, cells were incubated with BBR and BBR-NLCs (5 μg/mL) for 0.5, 1, or 2 h. The cells were washed with phosphate-buffered saline (PBS) and fixed with 4% paraformaldehyde for 15 min, then washed three times with cold PBS. Intracellular localization of BBR was visualized using a fluorescence microscope.

Caco-2 cells and RAW 264.7 cells (4×10^6 cells/well) were seeded in 6-well plates. On the next day, the cells were treated with BBR or BBR-NLCs (5 μg/mL) for 0.5, 1, or 2 h, then harvested for flow cytometry analysis.

Colitis Model Construction and Treatment Conditions

Wild-type Balb/c mice were purchased from the Experimental Animal Center of Southern Medical University (Certificate SCXK2016-0041). Thirty mice (weight, 22 ± 2 g) were randomly divided into the following five groups: control, DSS, NLCs, free BBR, and BBR-NLCs (n = 6 in each group).

All animal procedures were approved by the Committee on Animals of the Jinan University. All animal procedures were performed in accordance with the guidelines of the Committee on Animal of the Jinan University.

Acute colitis was induced as described previously.[28] Each group (except the control group) was continuously provided 2.5% DSS (molecular mass, 36–50 kDa; MP Biomedicals, Solon, Ohio, USA) in drinking water for 7 days, NLCs, free BBR, and BBR-NLCs were administered orally began following three days of drinking 2.5% DSS in water (Figure 1A). Mice in the control group received regular drinking water throughout the experiment. Drinking water containing 2.5% DSS was replaced every other day.

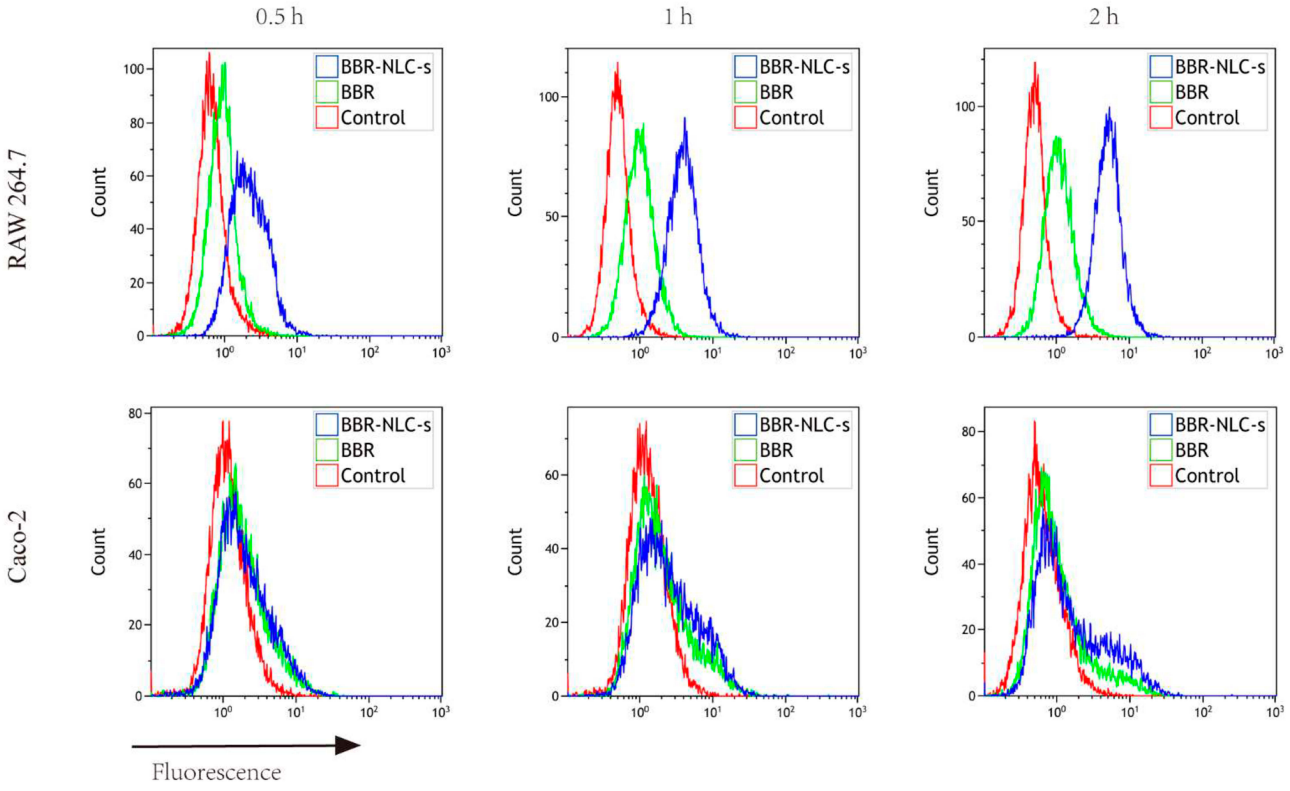

Figure 1 Uptake of BBR and BBR-NLCs into RAW264.7 and Caco-2 cells was evaluated for 0.5, 1, and 2 h.
Notes: Flow cytometry was used to quantify the fluorescence intensity. For all experiments, n = 3.

Disease Activity Index (DAI)

Body weight, stool characteristics, and blood in the stool were recorded daily and averaged to determine DAI. Each parameter was scored as follows: body weight loss (0, <1%; 1, 1–5%; 2, 5–10%; 3, 10–15%; 4, >15%), the presence or absence of blood in the feces (0, negative; 2, hidden blood in stool; 4, bloody stool), and stool consistency (0, negative; 2, loose stools; 4, diarrhea).[29]

Histological Score

Mice were sacrificed after drinking DSS for 7 days. The colons were collected, measured for length, and then washed with normal saline. The middle segments of the colons were fixed in 4% paraformaldehyde (Beyotime biotechnology, China) for 24 h, embedded in paraffin, sectioned into 4-μm slices, then stained with hematoxylin and eosin (H&E). Severity of inflammation was evaluated using a previously described scoring system.[30]

Myeloperoxidase (MPO) Measurement

The distal colons were weighed and homogenized in 0.1 M phosphate buffer (pH 7.4), then centrifuged at 10,000 rpm for 15 min at 4°C. Myeloperoxidase activity was measured in the supernatant using an MPO activity assay kit (Nanjing Jiancheng Biochemical Engineering, Nanjing, China). Myeloperoxidase activity was expressed as U/mg protein.[31]

Immunofluorescence Analyses

To study tight junction (TJ) proteins, colon sections were fixed with 4% formaldehyde for 24 h, permeabilized with 0.1% Triton X-100 for 10 min, blocked with 10% fetal bovine serum (FBS) for 30 min, then incubated with a primary antibody against zonula occludens-1 (ZO-1) (1:50; eBioscience, San Diego, USA) overnight at 4°C. After washing 3 times with PBS (5 min each time), the monolayer was incubated with Cy3-conjugated secondary antibodies in the dark for 1 h. The cells were then stained with 4′, 6-diamidino-2-phenylindole (DAPI) (Beyotime biotechnology, China) in the dark for 10 min, then washed 3 times. Cells on glass coverslips were mounted onto clean glass slides using fluorescence mounting media, and the cells were visualized using a fluorescence microscope (Nikon, Japan). Fluorescence intensity was determined using Image J 1.51 software.

We evaluated influence of BBR on nuclear factor-κB (NF-κB) nuclear translocation as described by Shan Han, with some modifications.[32] RAW264.7 cells were seeded in confocal dishes at a density of 1.5×10^5 cells/well and allowed to adsorb overnight. Cells were pretreated with BBR or BBR-NLCs (5 μg/mL) for 2 h, then stimulated with 100 ng/mL lipopolysaccharide (LPS; Sigma, St. Louis, MO) for 6 h. The cells were fixed, blocked, then incubated with anti-NF-κB p65 antibody (1:500; Santa Cruz Biotechnology, Dallas, TX, USA) overnight at 4°C. Then, the cells were incubated with AlexaFluor 594 secondary antibody for 1 h. Nuclei were stained with DAPI and visualized using a confocal microscope (LSM880; Carl Zeiss, Jena, Germany).

Quantitative Real-Time PCR to Determine the Expression of Inflammatory Substances

After incubation with or without 2% DSS for 48 h, cells were washed with 1X PBS, and total RNA was isolated with TRIzol Reagent (TIANGEN Biotech, Beijing, China). Complementary DNA was reverse transcribed using an IScript Advanced cDNA synthesis kit. Real-time PCR was performed using a Bio-Rad Real-Time PCR System with SYBR Green PCR Master Mix. Specific primers were synthesized by Shanghai Shenggong Biotechnology (Shanghai, China) (Table 1). The following thermal parameters were used for PCR:

Table 1 Quantitative Real-Time PCR Primer Sequence

Gene	Forward Primer	Reverse Primer
IL-1β	GAGCCTGTGTTTCCTCCTTG	CAAGTGCAAGGCTATGACCA
IL-6	CTGACAATATGAATGTTGGG	TCCAAGAAACCATCTGGCTAGG
MMP-9	GCAGAGGCATACTTGTACCG	TGATGTTATGATGGTCCCACTTG
COX-2	ATTCCAAACCAGCAGACTCATA	CTTGAGTTTGAAGTGGTAACCG
CX3CR1	TCTGTTGGTGGTCCTCGCTCTC	ATGAAGAAGAAGGCAGTCGTGAGC
TERT	CGGAAGAGTGTCTGGAGCAA	GGATGAAGCGGAGTCTGGA
β-Actin	GGCTGTATTCCCCTCCATCG	CCAGTTGGTAACAATGCCATGT

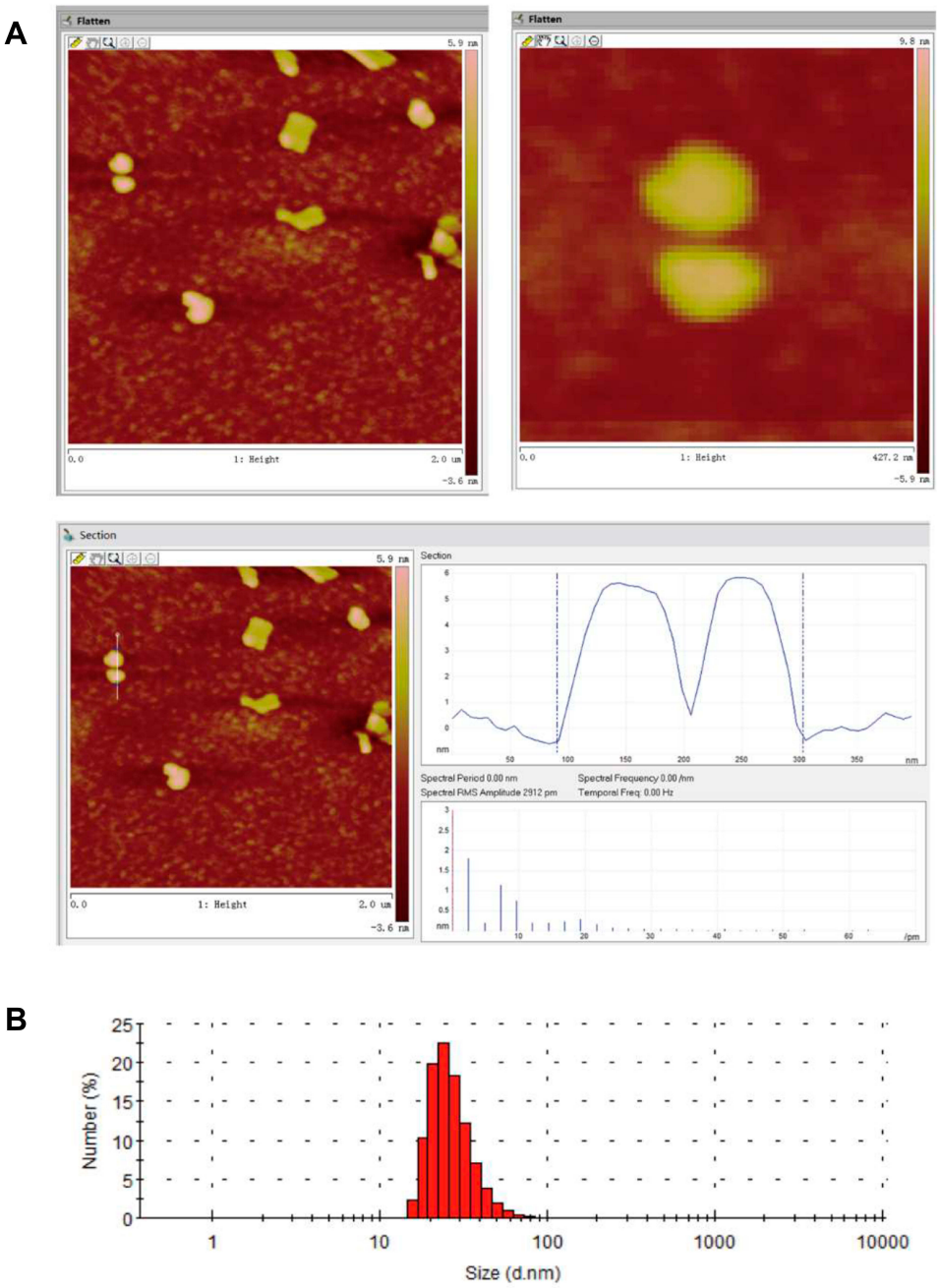

Figure 2 Characterization of BBR-NLCs.
Note: (**A**) AFM image and (**B**) size distribution.

50°C for 2 min, 95°C for 10 min, 40 cycles of amplification at 95°C for 15 s, and 60°C for 1 min.

Statistical Analysis

All data are expressed as the mean ± SD. Statistical analysis was performed using GraphPad Prism 7 software (San Diego, CA, USA). Data among groups were analyzed by one-way ANOVA. P-values < 0.05 were considered statistically significant.

Results

Characterization of BBR-NLCs

Nanostructured lipid carriers with a BBR concentration of 1 mg/mL were successfully prepared using high-pressure homogenization. As shown in Figure 2A, analysis of BBR-NLCs using AFM analysis resulted in 3D images and particle size determination (about 100 nm). Previous studies have shown that the deposited SLN on mica plates would be flattened slightly, likewise, the size of BBR-NLCs obtained

Table 2 Summary of Characterization of BBR-NLCs

Characterization	Value
Particle size	63.96± 0.31 nm
Polydispersity index	0.29 ± 0.01
Zeta potential	+3.16 ± 0.05 mV
Drug loading	6.00±0.09%
Entrapment efficiency	101.97±6.34%

from AFM would be greater than the true.[33] Results obtained from a Malvern ZetaSizer showed that the average particle size, PDI, zeta potential, drug loading and entrapment efficiency of BBR-NLCs were 63.96± 0.31 nm, 0.29 ± 0.01, +3.16 ± 0.05 mV, 6.00±0.09% and 101.97±6.34%, respectively (Figure 2B, Table 2). Dissolution profiles of BBR and BBR-NLCs in simulated gastric and intestinal juices are displayed in Figure 3. The dissolution profile of the BBR-NLCs showed that 11.31% of the drug had been released in 2 h, compared to 39.11% of the free BBR in simulated gastric fluid. In addition, the dissolution profile of the BBR-NLCs showed that 53.37% of the drug had been released in 4 h, compared to 73.39% of the free BBR in simulated intestinal fluid. A higher dissolution rate of BBR-NLCs was obtained in simulated intestinal fluid showed the nanostructured lipid carriers delivery system has great potential to develop as pH sensitive drug delivery systems, enhance the release of nano-drug at site of action.[34,35] These results indicated that BBR-NLCs were of appropriate quality for the intended use in this study.

Evaluation of BBR-NLCs Biocompatibility

We assessed the toxicity of BBR-NLCs in vivo. Normal mice were orally administered BBR-NLCs for 4 days. In Figure 4, three oral administration groups (NLCs, BBR and BBR-NLCs) are compared with control group, respectively. We determined no obvious toxicity of the three oral administration groups in vivo through the pathological results of heart, liver, spleen, lung, and kidney.

Evaluation of in vitro Cellular Uptake

Uptake of BBR-NLCs was evaluated in RAW264.7 and Caco-2 cells using fluorescence microscopy. Each cell line was treated with equivalent concentrations of free BBR and BBR-NLCs for 0.5, 1, and 2 h. Green fluorescence indicated BBR uptake. As shown in Figure 5, overlays of the two acquired channels showed the distribution of BBR in the nucleus and cytoplasm. Stronger fluorescence was observed in RAW264.7 cells in response to BBR-NLCs (Figure 5B, D and F) than that in response to BBR (Figure 5A, C and E). Similar results were observed in Caco-2 cells, in which BBR-NLCs were taken up to a greater extent than free BBR (Figure 5G–L). These findings were consistent with the previous observation that small molecules mainly diffuse into cells, while uptake of nanocarriers occurs through endocytosis.[36]

To verify the qualitative results, intracellular BBR content was quantified using flow cytometry. As shown in Figure 1, free BBR and BBR-NLCs were incubated with RAW 264.7 cells and Caco-2 cells for 0.5, 1, and 2 h. The results showed that BBR-NLCs were internalized to a greater extent than free BBR in RAW 264.7 and Caco-2 cells.

BBR-NLCs Attenuated DSS-Induced Acute Colitis

In this study, the protective effects of BBR and BBR-NLCs were evaluated in DSS-induced colitis model. Studies have shown that DSS breaks down the epithelial

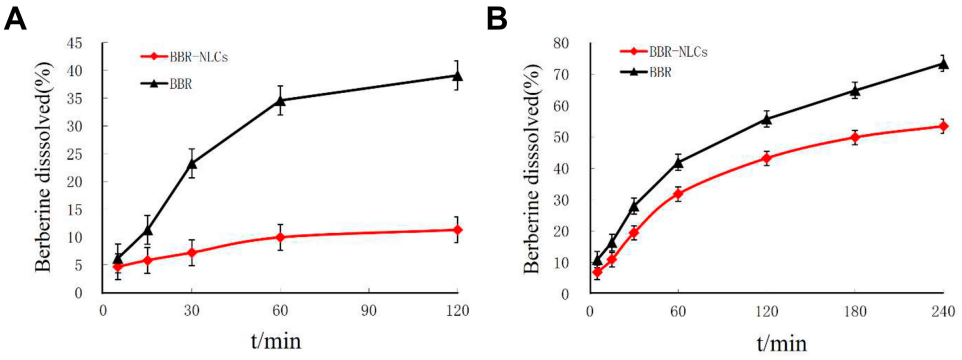

Figure 3 Dissolution profiles of BBR and BBR-NLCs.
Note: (**A**) In simulated gastric juice; (**B**) in simulated intestinal juice.

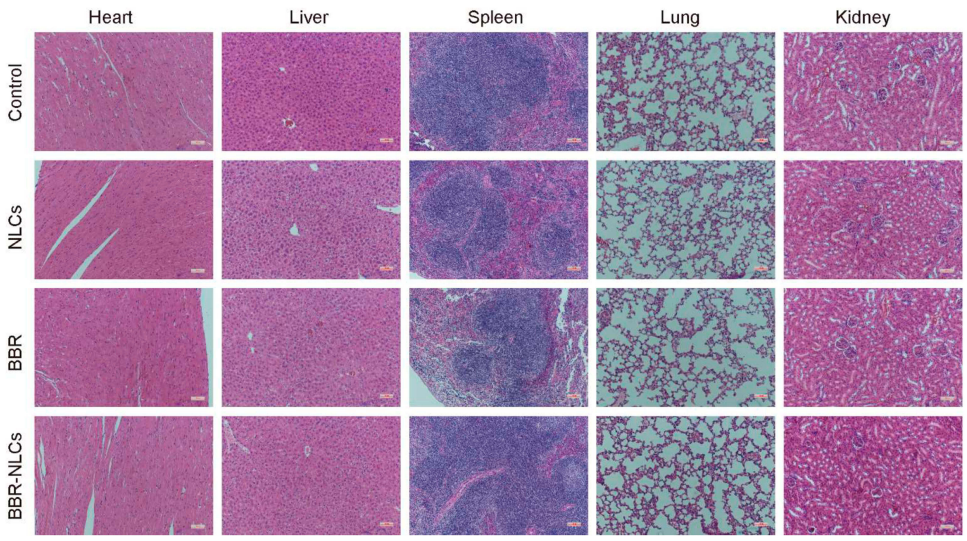

Figure 4 Hematoxylin and eosin staining of histological sections were used to assess the toxicity of BBR-NLCs toward major organs (heart, liver, spleen, lung, and kidney).

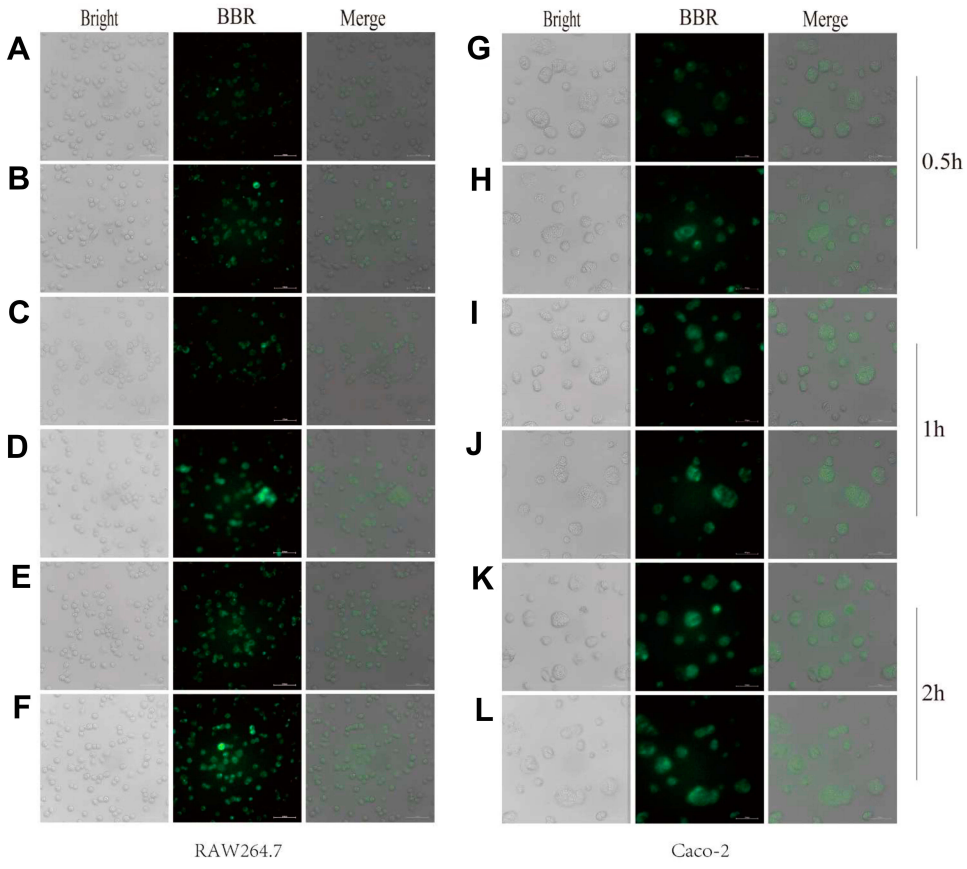

Figure 5 Uptake of berberine (BBR) and BBR-NLCs into RAW264.7 and Caco-2 cells were evaluated for 0.5 (**A, B, G, H**), 1 (**C, D, I, J**), and 2 h (**E, F, K, L**).
Notes: The cell outline in each plane was determined using bright field imaging. BBR fluoresces (green channel), which allowed for tracking without modification of the drug. For all experiments, n = 3, and the scale bar = 100 μm.

barrier to induce UC, which results in weight loss, diarrhea, occult blood in stools, piloerection, anemia, and eventually death.[37] Mice were sacrificed on the eighth day, and the severity of inflammation was assessed using DAI, colon length, and macro-level histology. As shown in Figure 6B, DSS resulted in increased DAI,

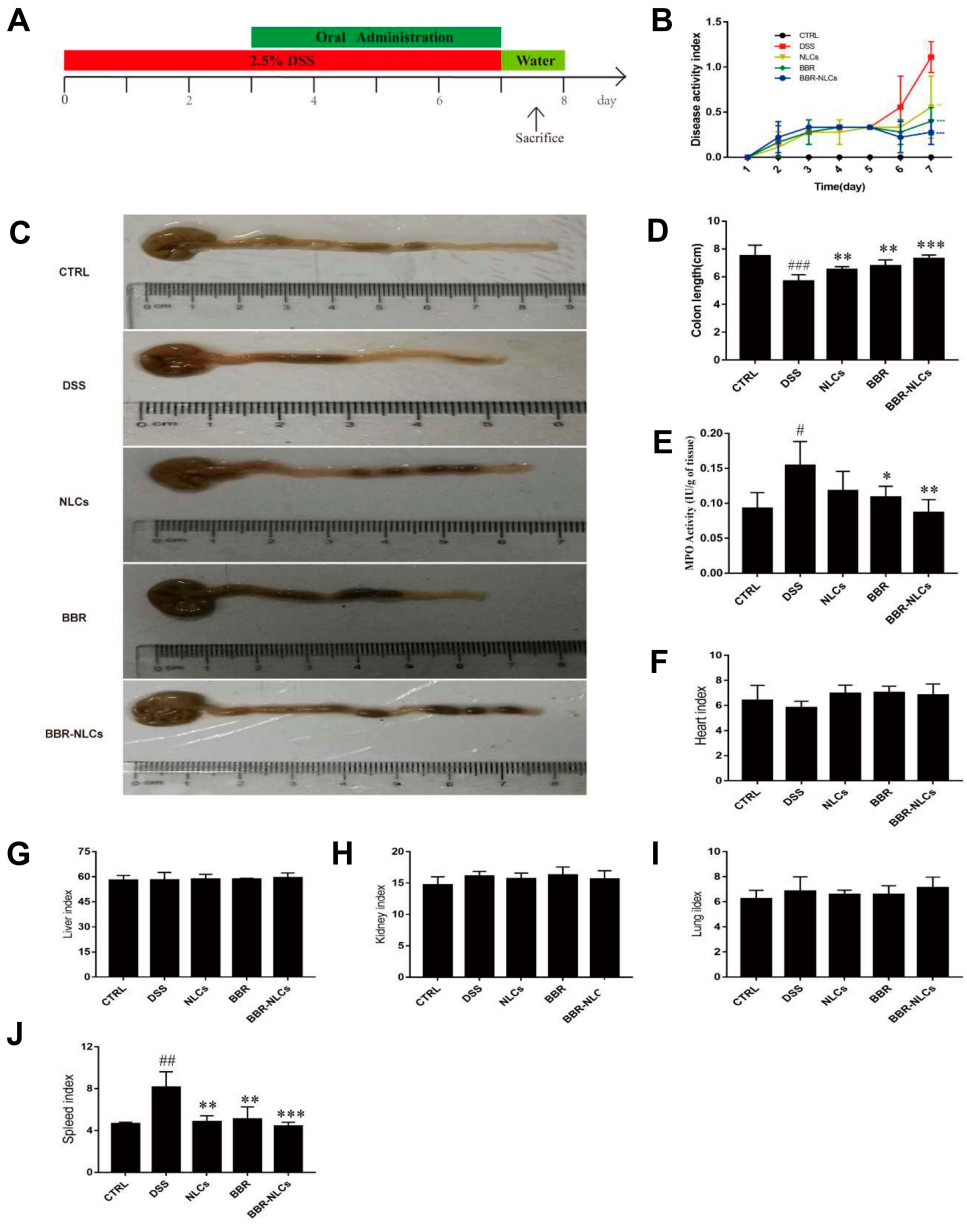

Figure 6 Treatment with BBR-NLCs alleviated symptoms of DSS-induced experimental colitis in mice.

Notes: (**A**) Experimental protocol for DSS-induced colitis in mice. (**B**) Determination of DAI. (**C**) Representative colon length in each group. (**D**) Statistical analysis of colon length. (**E**) Colon MPO activity. (**F**) Heart weight index. (**G**) Liver weight index. (**H**) Kidney weight index. (**I**) Lung weight index. (**J**) Spleen weight index. Data are presented as mean ± SD (n = 6). $^{\#}P < 0.05$, $^{\#\#}P < 0.01$, $^{\#\#\#\#}P < 0.001$ compared with the control group; $^{*}p < 0.05$, $^{**}p < 0.01$, $^{***}p < 0.001$ compared with the DSS group.

which correlated with development of UC. Oral administration of NLCs (0.55±0.34), free BBR (0.40±0.15), and BBR-NLCs (0.28±0.14) significantly attenuated diarrhea and occult blood compared to the DSS group (1.11±0.17). Furthermore, each treatment group blocked colon shortening and spleen swelling caused by DSS (Figure 6C and J). No differences in organ indices were found for the heart, liver, lung, and kidney among the groups (Figure 6E–I). Myeloperoxidase activity was lower in the free BBR group and BBR-NLCs group than that in the DSS group (Figure 6D). Treatment with BBR-NLCs provided more potent protective effects against UC than free BBR, which agreed with the in vitro uptake result in this study.

Histological Assessment of Colon Tissues

The histological characteristics of the colons of mice with DSS-induced colitis were assessed using H&E staining. Representative results and microscopic scores are summarized in Figure 7. Inflammatory cell

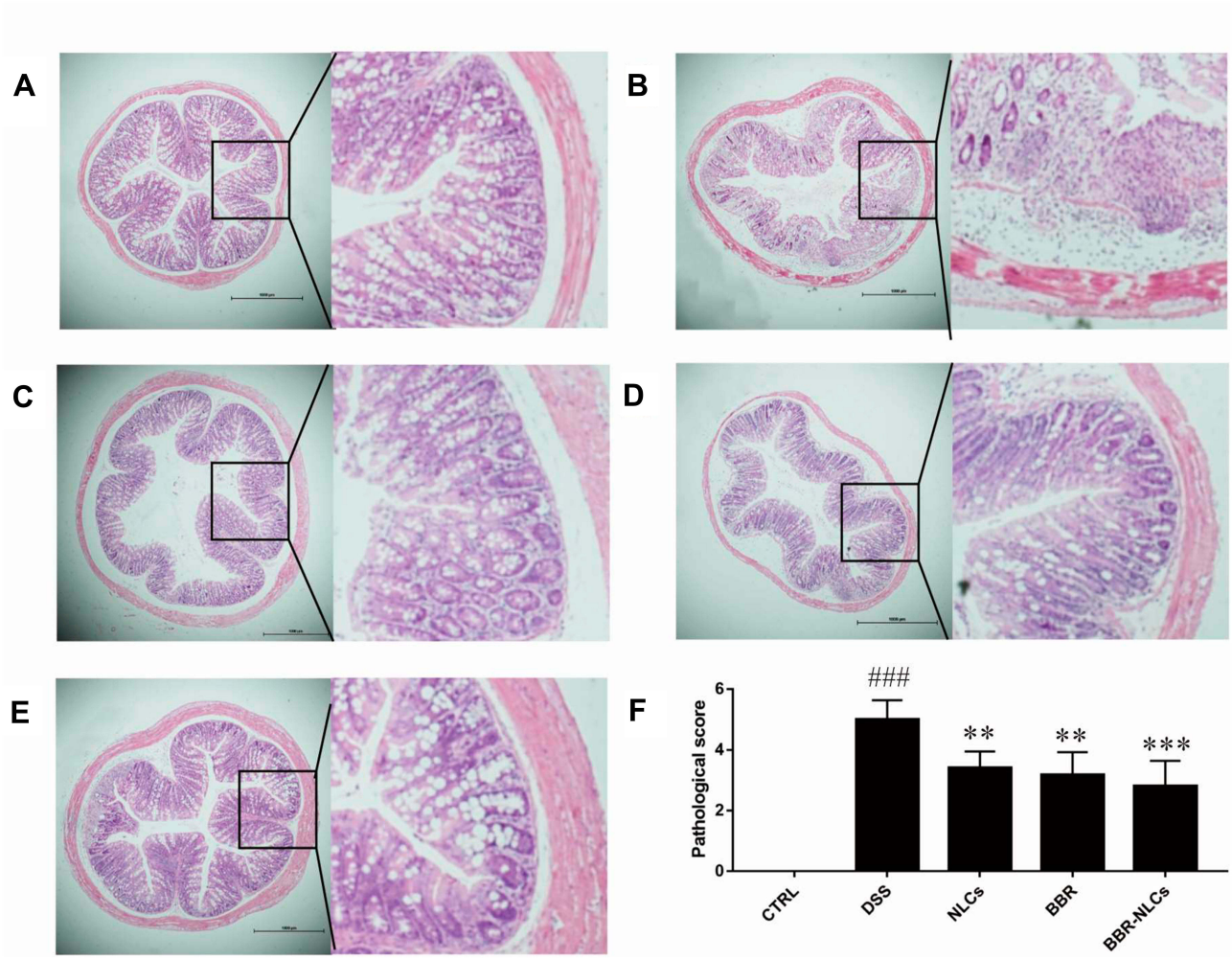

Figure 7 Representative colon tissue sections stained with hematoxylin and eosin visualized using a microscope.
Notes: (**A**) control; (**B**) DSS; (**C**) NLCs; (**D**) BBR; (**E**) BBR-NLCs. (**F**) Colitis histological score for each group. The scale bar = 1000 μm. Data are expressed as mean ± SD (n = 6). $^{###}P < 0.001$ compared with the control group; $^{**}p < 0.01$, $^{***}p < 0.001$ compared with the DSS group.

infiltration, edema, and changes in mucosal structure were observed in the DSS group. Treatment with NLCs, BBR, and BBR-NLCs ameliorated DSS-induced damage to crypt structures and severe inflammation, and this protective effect was most pronounced in response to treatment with BBR-NLCs.

Treatment with BBR-NLCs Blocked DSS-Induced ZO-1 Disruption

Immunofluorescence was used to evaluate the expression of ZO-1 (Figure 8). Treatment with free BBR and BBR-NLCs reversed DSS-induced decreases in the expression of ZO-1. These results showed that BBR and BBR-NLCs protected intestinal barrier function, and BBR-NLCs exerted more potent protective effects.

Inhibition of Colon Inflammation by BBR-NLCs

The expression levels of inflammatory mediators in the colon were measured to evaluate the protective effects of BBR-NLCs against DSS-induced UC (Figure 9). The expression levels of the pro-inflammatory genes interleukin-1 beta (IL-1β), interleukin 6 (IL-6), matrix metalloprotein 9 (MMP-9), chemokine (C-X3-C motif) receptor 1 (CX_3CR1), cyclooxygenase-2 (COX-2), and telomerase reverse transcriptase (TERT) were increased in the DSS group compared to those in the control group. Treatment with free BBR and BBR-NLCs significantly inhibited DSS-induced increases in expression of inflammatory mediators, and BBR-NLCs induced a more potent protective effect than free BBR.

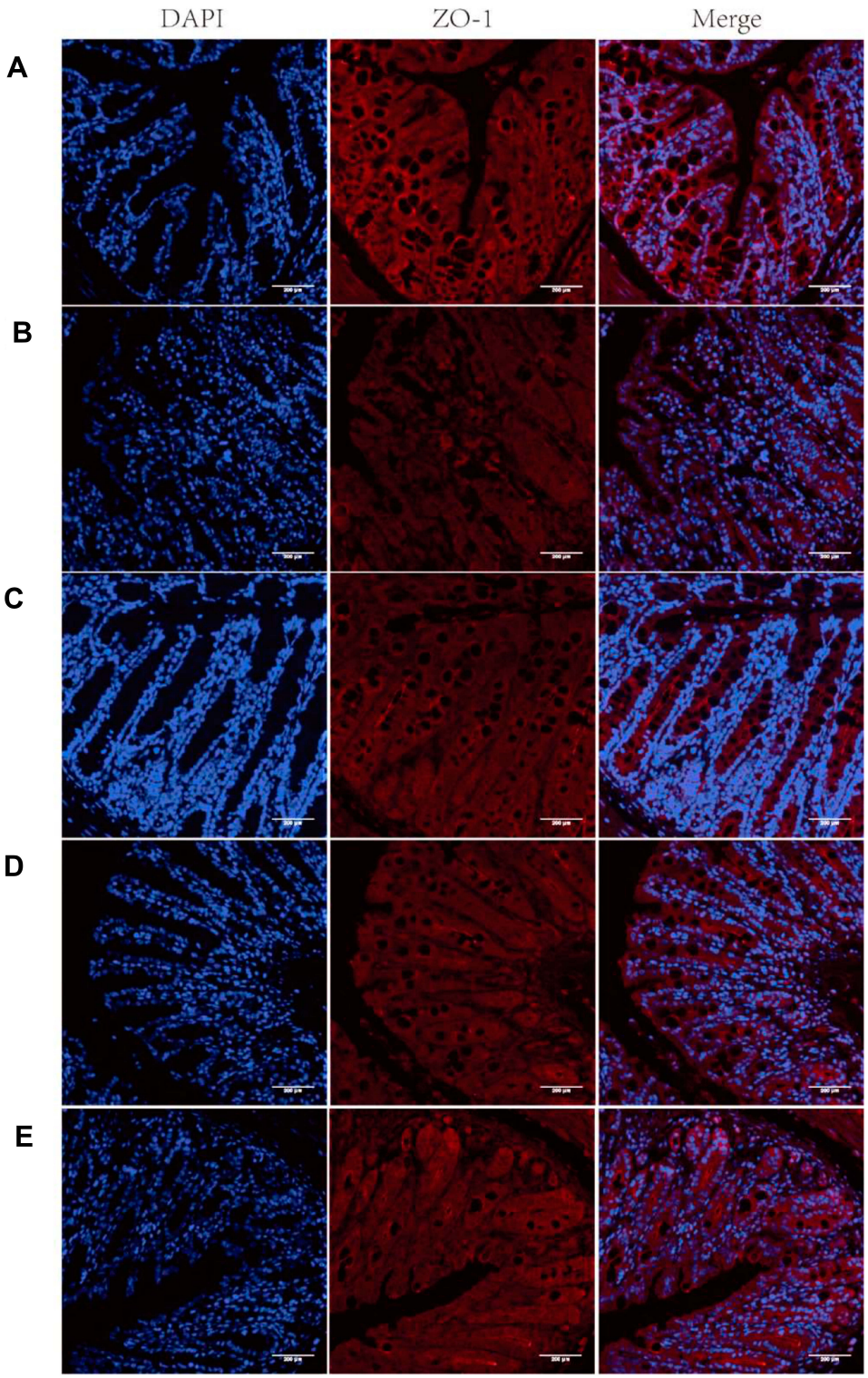

Figure 8 Representative images of ZO-1 immunofluorescence.
Notes: (**A**) Control; (**B**) DSS; (**C**) NLCs; (**D**) BBR; (**E**) BBR-NLCs. The tight junction protein ZO-1 was stained red, and nuclei were counterstained blue. The scale bar = 200 μm.

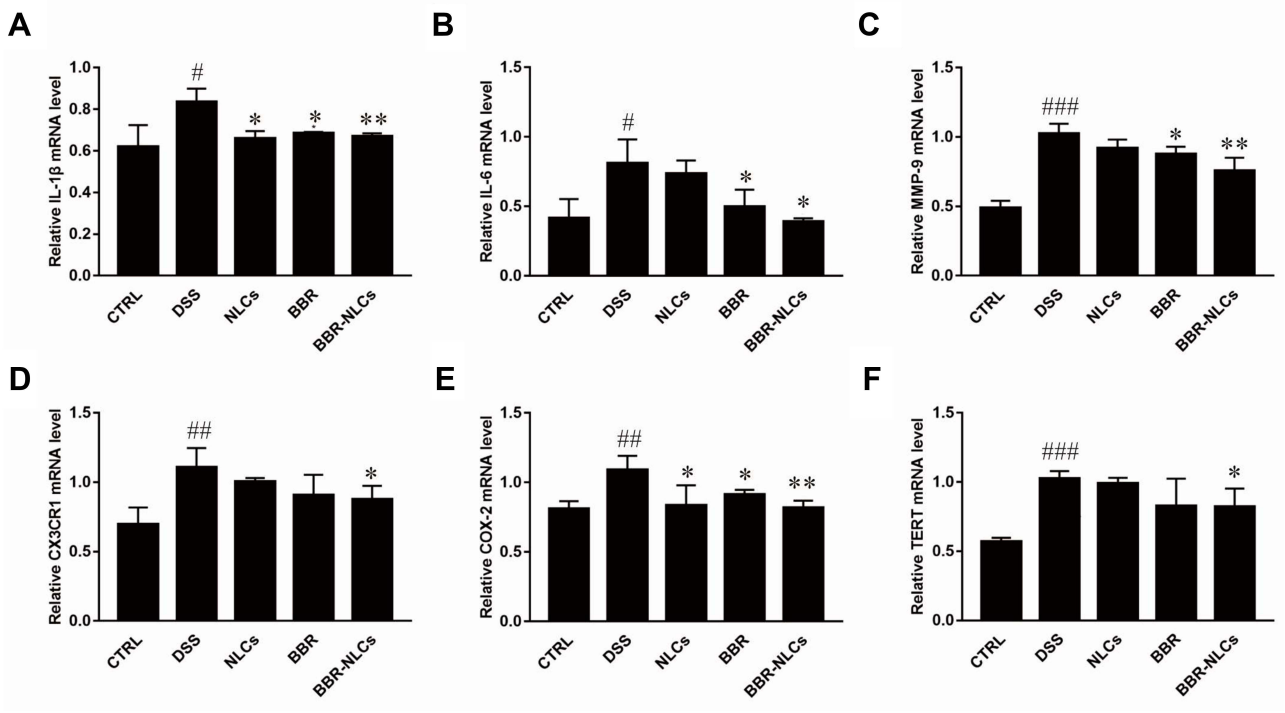

Figure 9 Suppression of mRNA expression of pro-inflammatory mediators in colon tissues in response to BBR and BBR-NLCs in mice with DSS-induced colitis in mice. **Notes:** (**A**) IL-1β; (**B**) IL-6; (**C**) MMP-9; (**D**) CX3CR1; (**E**) COX-2; and (**E**) TERT. Data are expressed as mean ± SD (n = 6). $^{\#}P<0.05$, $^{\#\#}P<0.01$, $^{\#\#\#}P < 0.001$ compared with the control group; *p < 0.05, **p < 0.01 compared the DSS group.

BBR-NLCs Suppressed LPS-Induced NF-κB Nuclear Translocation

Previous studies have shown that NF-κB is a key mediator of pro-inflammatory gene transcription.[38] Inactive NF-κB is bound to IκBα in the cytoplasm. Stimulation with LPS results in phosphorylation and degradation of IκBα, which allows nuclear translocation of NF-κB.[39] Immunofluorescence analyses indicated that LPS successfully induced translocation of NF-κB from cytoplasm to nucleus (Figure 10B), and that free BBR and BBR-NLCs significantly inhibited LPS-induced nuclear translocation of NF-κB (Figure 10C and D). In addition, treatment with BBR-NLCs resulted in levels of nuclear NF-κB similar to those in the control group (Figure 10A).

Discussion

Conventional drugs used to treat UC exhibit limited efficacy or induce severe adverse reactions.[5] Increasing numbers of studies have shown that natural products have great potential for the treatment of UC.[40,41] However, low bioavailability has limited the clinical use of natural products.[42] It is reported that pharmacists have applied nano-delivery systems to the delivery of natural drugs and developed many novel drug forms for the inflammatory bowel disease, skin diseases, and neurodegenerative diseases.[43–45]

In this study, we prepared BBR-NLCs using high-pressure homogenization to improve uptake of BBR and compared the anti-inflammatory effects of BBR-NLCs with those of free BBR. The characteristics of BBR-NLCs are summarized in Figure 2 and Table 2. The prepared BBR-NLCs ranged from 30 nm to 200 nm in size, which was optimal for cellular uptake.[46] Evaluation of biocompatibility of BBR-NLCs showed no apparent toxicity against major organs in vivo, which showed that BBR-NLCs were safe for use to treat UC.[47] Studies have shown that nanoscale drugs were taken up to a greater extent than free drugs.[48,49] In our uptake study, BBR-NLCs showed superior uptake compared with free BBR (Figures 1 and 5). In addition, qualitative analysis of uptake in vitro showed that BBR was distributed in the cytoplasm and nucleus, which was consistent with the findings of a study by Serafim.[50] Treatment with BBR-NLCs markedly improved DAI, colon length, MPO activity, spleen swelling, and histological characteristics of mice with DSS-induced UC, and this effect was stronger than that induced by free BBR (Figures 6 and 7). These results agreed with those from a study by Juntao Yin et al that showed that BBR-loaded NLCs enhanced the anti-

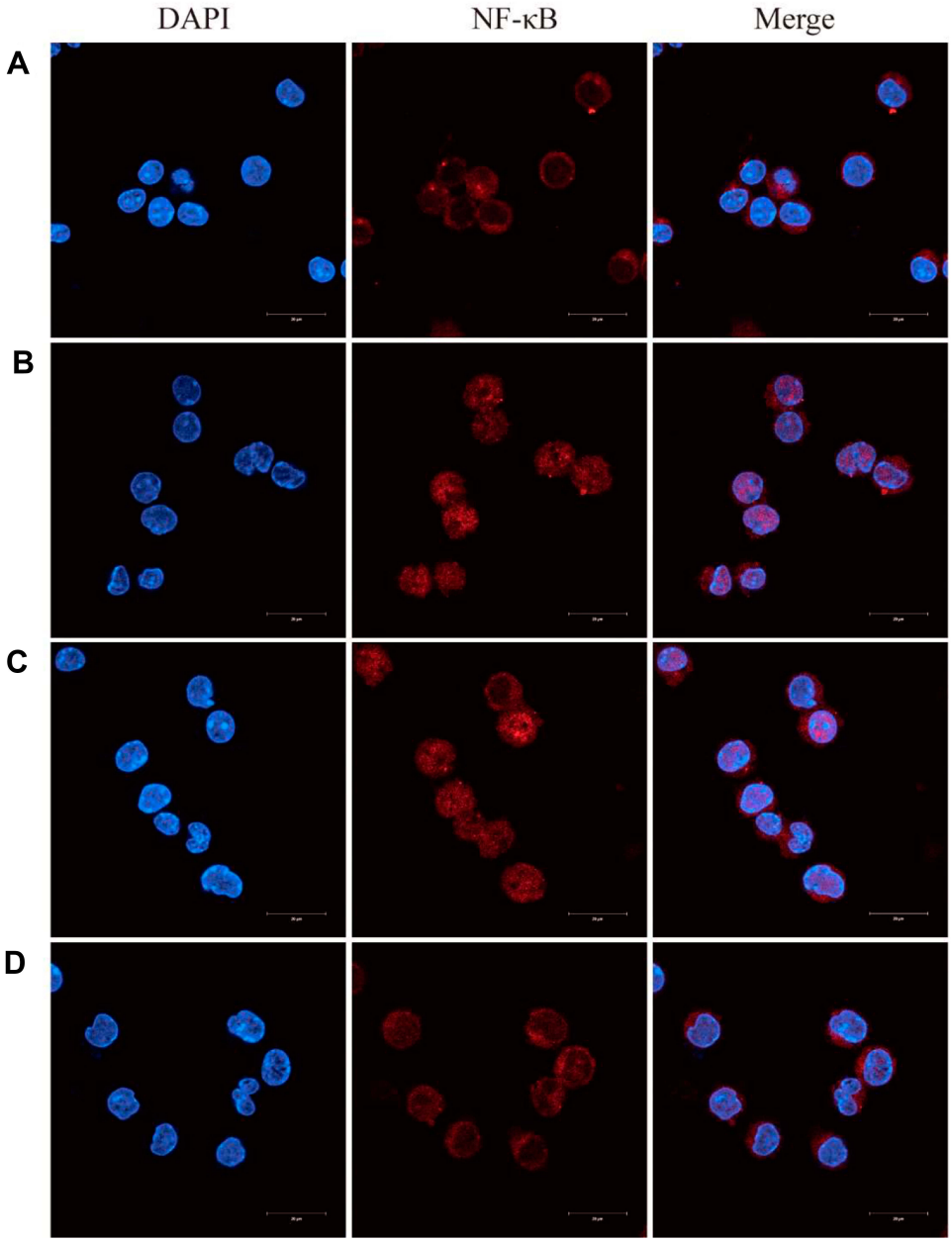

Figure 10 Berberine (BBR)-NLCs blocked LPS-induced NF-κB nuclear translocation.
Notes: (**A**) Untreated RAW264.7 cells. (**B**) RAW264.7 cells treated with LPS (100 ng/mL) for 6 h. (**C**) RAW264.7 cells pretreated with BBR (5 μg/mL) for 2 h, then treated with LPS (100 ng/mL) for 6 h. (**D**) RAW264.7 cells pretreated with BBR-NLCs (5 μg/mL) for 2 h, then treated with LPS (100 ng/mL) for 6 h. The translocation of NF-κB was determined using immunofluorescence. For all experiments, n = 3, and the scale bar = 20 μm.

diabetic activity of BBR.[51] These results were consistent with the advantages of nanostructured lipid carriers for drug delivery. Furthermore, treatment with nanostructured lipid carriers without drug also mitigated UC. Further investigation found that olive oil, a component of nanostructured lipid carriers, reduced inflammation in rats with DSS-induced colitis.[52] Therefore, olive oil may function as a drug delivery carrier and as an auxiliary therapeutic agent.

The mechanisms of the protective effects of BBR and BBR-NLCs against UC were investigated. BBR and BBR-NLCs inhibited pro-inflammatory gene expression (IL-1β, IL-6, COX-2, and TERT), and neutrophilic chemotaxis (MMP-9 and CX3CR1). Each of the pro-inflammatory genes evaluated in this study was associated with the NF-κB pathway.[53–56] Furthermore, BBR and BBR-NLCs inhibited translocation of NF-κB from the cytoplasm to the nucleus.

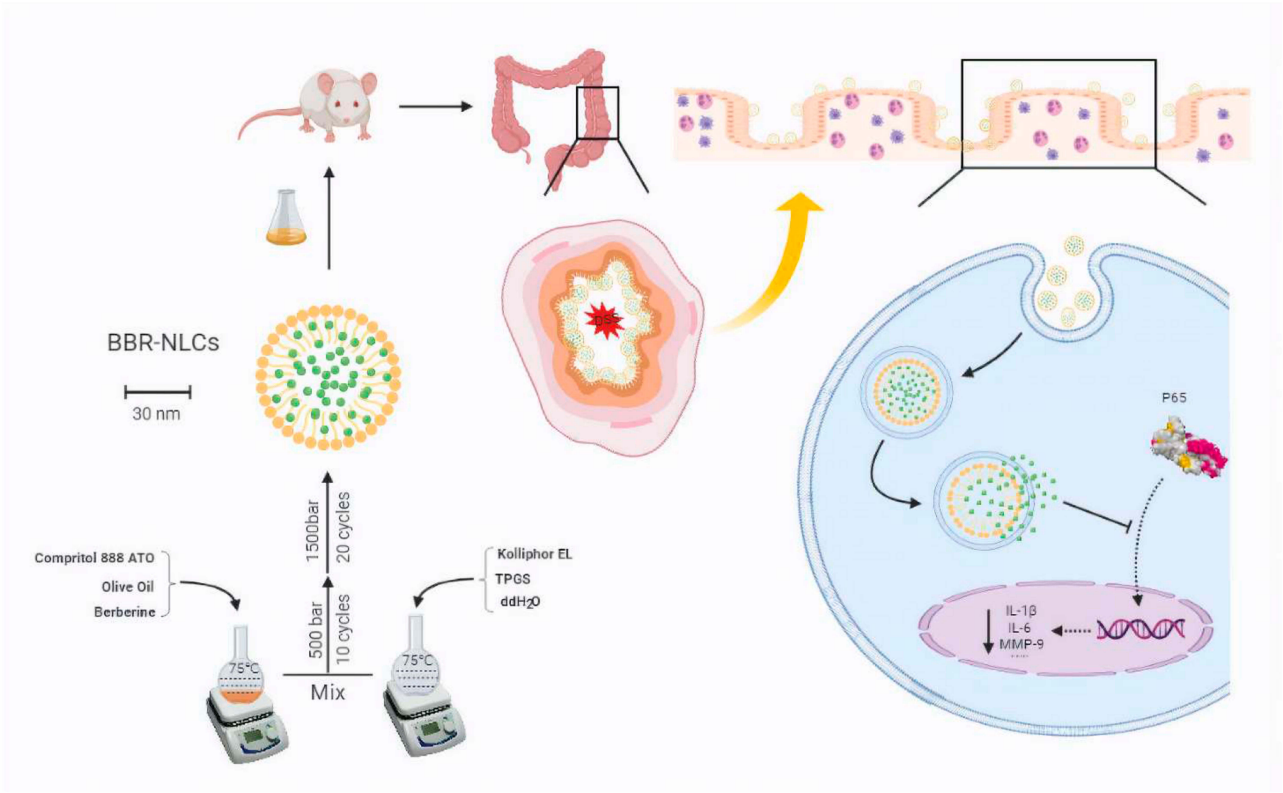

Figure 11 Schematic of preparation and functional mechanisms of BBR-NLCs.
Note: Image produced using BioRender.

Moreover, colon sections showed that the intestinal mucosal structure remained intact following treatment with BBR-NLCs. Immunofluorescence was used to evaluate the tight junction protein ZO-1 in colon tissue. The results showed that BBR-NLCs protected against UC-induced decreases in ZO-1 expression to a greater extent than free BBR. Our results showed that BBR-NLCs protected against UC to a greater extent than free BBR through inhibition of the NF-κB pathway. Preparation of BBR-NLCs and the associated protective mechanisms against UC are summarized in Figure 11.

Conclusion

In this study, we developed a novel method for preparation of BBR-NLCs. We showed that BBR-NLCs protected against inflammation associated with DSS-induced UC in mice through inhibition of the NF-κB pathway, which resulted in protection of the colon mucosa. These findings showed that BBR-NLCs may have potential as novel therapeutic agents for treatment of UC.

Acknowledgments

This work was supported by Guangdong Provincial Engineering Center of Topical Precise Drug Delivery System and the science and technology projects of Guangdong Province (2016A040402033); National Engineering Research Center for Modernization of Traditional Chinese Medicine Moxa herb Branch; Introduction of Leading Talents Program of Huizhou City; Technology Innovation Team Program of Huizhou City (20170217013144015); Daya Bay Technology Project (2017008). The Key Laboratory of Bioengineering Drugs of Guangdong Province of China; the Innovation Strong School Project of Department of Education of Guangdong Province and Guangdong Pharmaceutical University, China; the Talent Training Program of Guangdong Province Joint Training Graduate Demonstration Base.

Disclosure

The authors report no conflicts of interest in this work.

References

1. Ungaro R, Mehandru S, Allen PB, Peyrin-Biroulet L, Colombel J-F. Ulcerative colitis. *Lancet*. 2017;389:1756–1770. doi:10.1016/S0140-6736(16)32126-2
2. Antoni L, Nuding S, Wehkamp J, Stange EF. Intestinal barrier in inflammatory bowel disease. *World J Gastroenterol*. 2014;20(5):1165–1179. doi:10.3748/wjg.v20.i5.1165

3. Sharara AI, Awadhi SA, Alharbi O, et al. Epidemiology, disease burden, and treatment challenges of ulcerative colitis in Africa and the Middle East. *Expert Rev Gastroenterol Hepatol*. 2018;12(9):883–897. doi:10.1080/17474124.2018.1503052
4. Jacques C, Corinne G-R, Philippe S, Antoine C. Epidemiology and natural history of inflammatory bowel diseases. *Gastroenterology*. 2011;140(6):1785–1794. doi:10.1053/j.gastro.2011.01.055
5. Panes J, Alfaro I. New treatment strategies for ulcerative colitis. *Expert Rev Clin Immunol*. 2017;13(10):963–973. doi:10.1080/1744666X.2017.1343668
6. Suntar I, Cevik CK, Ceribasi AO, Gokbulut A. Healing effects of Cornus mas L. in experimentally induced ulcerative colitis in rats: from ethnobotany to pharmacology. *J Ethnopharmacol*. 2020;248:112322. doi:10.1016/j.jep.2019.112322
7. Batista JA, Magalhaes DDA, Sousa SG, et al. Polysaccharides derived from Morinda citrifolia Linn reduce inflammatory markers during experimental colitis. *J Ethnopharmacol*. 2020;248:112303. doi:10.1016/j.jep.2019.112303
8. Akkol EK, Dereli FTG, Tastan H, Sobarzo-Sanchez E, Khan H. Effect of Sorbus domestica and its active constituents in an experimental model of colitis rats induced by acetic acid. *J Ethnopharmacol*. 2019;251:112521. doi:10.1016/j.jep.2019.112521
9. Alabi QK, Akomolafe RO, Omole JG, et al. Polyphenol-rich extract of Ocimum gratissimum leaves ameliorates colitis via attenuating colonic mucosa injury and regulating pro-inflammatory cytokines production and oxidative stress. *Biomed Pharmacother*. 2018;103:812–822. doi:10.1016/j.biopha.2018.04.071
10. Lin CH, Chen CH, Lin ZC, Fang JY. Recent advances in oral delivery of drugs and bioactive natural products using solid lipid nanoparticles as the carriers. *J Food Drug Anal*. 2017;25(2):219–234. doi:10.1016/j.jfda.2017.02.001
11. Ma C, Battat R, Dulai PS, et al. Innovations in oral therapies for inflammatory bowel disease. *Drugs*. 2019;79(12):1321–1335. doi:10.1007/s40265-019-01169-y
12. Gao C, Liu L, Zhou Y, Bian Z, Wang S, Wang Y. Novel drug delivery systems of Chinese medicine for the treatment of inflammatory bowel disease. *Chin Med*. 2019;14:23. doi:10.1186/s13020-019-0245-x
13. Habtemariam S. Berberine and inflammatory bowel disease: a concise review. *Pharmacol Res*. 2016;113:592–599. doi:10.1016/j.phrs.2016.09.041
14. Liu S, Lee H, Hung C, Tsai C, Li T, Tang C. Berberine attenuates CCN2-induced IL-1β expression and prevents cartilage degradation in a rat model of osteoarthritis. *Toxicol Appl Pharmacol*. 2015;289:20–29. doi:10.1016/j.taap.2015.08.020
15. Cheng F, Wang Y, Li J, et al. Berberine improves endothelial function by reducing endothelial microparticles-mediated oxidative stress in humans. *Int J Cardiol*. 2013;167(3):936–942. doi:10.1016/j.ijcard.2012.03.090
16. Chang W, Chen L, Hatch GM. Berberine as a therapy for type 2 diabetes and its complications: from mechanism of action to clinical studies. *Biochem Cell Biol*. 2015;93(5):479–486. doi:10.1097/MD.0000000000016947
17. Mirhadia E, Rezaeeb M, Nikouei BM. Nano strategies for berberine delivery, a natural alkaloid of Berberis. *Biomed Pharmacother*. 2018;104:465–473. doi:10.1016/j.biopha.2018.05.067
18. Yu F, Li M, Yuan Z, et al. Mechanism research on a bioactive resveratrol- PLA-gelatin porous nano-scaffold in promoting the repair of cartilage defect. *Int J Nanomedicine*. 2018;13:7845–7858. doi:10.2147/IJN.S181855
19. Ibrahim S, Tagami T, Kishi T, Ozeki T. Curcumin marinosomes as promising nano-drug delivery system for lung cancer. *Int J Pharm*. 2018;540:40–49. doi:10.1016/j.ijpharm.2018.01.051
20. Wang L, Feng M, Li Y, et al. Fabrication of superparamagnetic nano-silica@ quercetin-encapsulated PLGA nanocomposite: potential application for cardiovascular diseases. *J Photochem Photobiol B*. 2019;196:111508. doi:10.1016/j.jphotobiol.2019.05.005
21. Saedi A, Rostamizadeh K, Parsa M, Dalali N, Ahmadi N. Preparation and characterization of nanostructured lipid carriers as drug delivery system: influence of liquid lipid types on loading and cytotoxicity. *Chem Phys Lipids*. 2018;216:65–72. doi:10.1016/j.chemphyslip.2018.09.007
22. Behbahani ES, Ghaedi M, Abbaspour M, Rostamizadeh K. Optimization and characterization of ultrasound assisted preparation of curcumin-loaded solid lipid nanoparticles: application of central composite design, thermal analysis and X-ray diffraction techniques. *Ultrason Sonochem*. 2017;38:271–280. doi:10.1016/j.ultsonch.2017.03.013
23. Yang B, Jiang J, Jiang L, et al. Chitosan mediated solid lipid nanoparticles for enhanced liver delivery of zedoary turmeric oil in vivo. *Int J Biol Macromol*. 2020;149:108–115. doi:10.1016/j.ijbiomac.2020.01.222
24. Yu Q, Hu X, Ma Y, et al. Lipids-based nanostructured lipid carriers (NLCs) for improved oral bioavailability of sirolimus. *Drug Deliv*. 2016;23(4):1469–1475. doi:10.3109/10717544.2016.1153744
25. Montoto SS, Sbaraglini ML, Talevi A, et al. Carbamazepine-loaded solid lipid nanoparticles and nanostructured lipid carriers: physicochemical characterization and in vitro/in vivo evaluation. *Colloids Surf B Biointerfaces*. 2018;167:73–81. doi:10.1016/j.colsurfb.2018.03.052
26. Fathi HA, Allam A, Elsabahy M, Fetih G, El-Badry M. Nanostructured lipid carriers for improved oral delivery and prolonged antihyperlipidemic effect of simvastatin. *Colloids Surf B Biointerfaces*. 2018;162:236–245. doi:10.1016/j.colsurfb.2017.11.064
27. Zhang Y, Cui Y, Gao L, Jiang H. Effects of β-cyclodextrin on the intestinal absorption of berberine hydrochloride, a P-glycoprotein substrate. *Int J Biol Macromol*. 2013;59:363–371. doi:10.1016/j.ijbiomac.2013.04.074
28. Jadert C, Phillipson M, Holm L, Lundberg JO, Borniquel S. Preventive and therapeutic effects of nitrite supplementation in experimental inflammatory bowel disease. *Redox Biol*. 2014;2:73–81. doi:10.1016/j.redox.2013.12.012
29. Lian L, Zhang S, Yu Z, et al. The dietary freeze-dried fruit powder of Actinidia arguta ameliorates dextran sulphate sodium-induced ulcerative colitis in mice by inhibiting the activation of MAPKs. *Food Funct*. 2019;10(9):5768–5778. doi:10.1039/C9FO00664H
30. Zhang Z, Li S, Cao H, et al. The protective role of phloretin against dextran sulfate sodium-induced ulcerative colitis in mice. *Food Funct*. 2019;10(1):422–431. doi:10.1039/c8fo01699b
31. Valero MS, González M, Ramón-Gimenez M, et al. Jasonia glutinosa (L.) DC., a traditional herbal medicine, reduces inflammation, oxidative stress and protects the intestinal barrier in a murine model of colitis. *Inflammopharmacology*. 2019;2019:1–18. doi:10.1007/s10787-019-00626-0
32. Han S, Gao H, Chen S, et al. Procyanidin A1 alleviates inflammatory response induced by LPS through NF-κB, MAPK, and Nrf2/HO-1 pathways in RAW264.7 cells. *Sci Rep*. 2019;9:15087. doi:10.1038/s41598-019-51614-x
33. Chen H, Chang X, Du D, et al. Podophyllotoxin-loaded solid lipid nanoparticles for epidermal targeting. *J Control Release*. 2006;110(2):296–306. doi:10.1016/j.jconrel.2005.09.052
34. Rui H, Hua Z, Cao J, Davoudi Z, Wang Q. Synthesis and in vitro characterization of carboxymethyl chitosan-CBA-doxorubicin conjugate nanoparticles as pH-sensitive drug delivery systems. *J Biomed Nanotechnol*. 2017;13(9):1097–1105. doi:10.1166/jbn.2017.2407
35. Hu R, Zheng H, Cao J, Davoudi Z, Wang Q. Self-assembled hyaluronic acid nanoparticles for pH-sensitive release of doxorubicin: synthesis and in vitro characterization. *J Biomed Nanotechnol*. 2017;13(9):1058–1068. doi:10.1166/jbn.2017.2406
36. Zheng Y, Lv X, Xu Y, Cheng X, Wang X, Tang R. pH-sensitive and pluronic-modified pullulan nanogels for greatly improved antitumor in vivo. *Int J Biol Macromol*. 2019;139:277–289. doi:10.1016/j.ijbiomac.2019.07.220
37. Martina P, Cerar A. Dextran sodium sulphate colitis mouse model: traps and tricks. *J Biomed Biotechnol*. 2012;2012:718617. doi:10.1155/2012/718617

38. Lawrence T. The nuclear factor NF-kappaB pathway in inflammation. *Cold Spring Harb Perspect Biol*. 2009;1(6):1–10. doi:10.1101/cshperspect.a001651
39. Liu Y, Kim S, Kim YJ, et al. Green synthesis of gold nanoparticles using leaf extract to inhibit lipopolysaccharide-induced inflammation through NF-κB and JAK/STAT pathways in RAW 264.7 macrophages. *Int J Nanomedicine*. 2019;14:2945–2959. doi:10.2147/IJN.S199781
40. He W, Liu M, Li Y, et al. Flavonoids from Citrus aurantium ameliorate TNBS-induced ulcerative colitis through protecting colonic mucus layer integrity. *Eur J Pharmacol*. 2019;857:172456. doi:10.1016/j.ejphar.2019.172456
41. Shen H, Xue J, Li T, et al. Ginseng polysaccharides enhanced ginsenoside Rb1 and microbial metabolites exposure through enhancing intestinal absorption and affecting gut microbial metabolism. *J Ethnopharmacol*. 2018;216:47–56. doi:10.1016/j.jep.2018.01.021
42. Watkins R, Wu L, Zhang C, Davis RM, Xu B. Natural product-based nanomedicine: recent advances and issues. *Int J Nanomedicine*. 2015;10:6055–6074. doi:10.2147/IJN.S92162
43. Carter P, Narasimhan B, Wang Q. Biocompatible nanoparticles and vesicular systems in transdermal drug delivery for various skin diseases. *Int J Pharm*. 2019;555:49–62. doi:10.1016/j.ijpharm.2018.11.032
44. Poovaiah N, Davoudi Z, Peng H, et al. Treatment of neurodegenerative disorders through the blood–brain barrier using nanocarriers. *Nanoscale*. 2018;10:16962–16983. doi:10.1039/C8NR04073G
45. Davoudi Z, Peroutka-Bigus N, Bellaire B, Wannemuehler M, Wang Q. Intestinal organoids containing PLGA nanoparticles for the treatment of inflammatory bowel diseases. *J Biomed Mater Res A*. 2017;106(4):876–886. doi:10.1002/jbm.a.36305
46. Hajipour H, Hamishehkar H, Ahmad SNS, Barghi S, Maroufi NF, Taheri RA. Improved anticancer effects of epigallocatechin gallate using RGD-containing nanostructured lipid carriers. *Artif Cells Nanomed Biotechnol*. 2018;46(sup1):283–292. doi:10.1080/21691401.2017.1423493
47. Zhang M, Xu C, Wang L, Merlin D. Oral delivery of nanoparticles loaded with ginger active compound, 6-shogaol, attenuates ulcerative colitis and promotes wound healing in a murine model of ulcerative colitis. *J Crohns Colitis*. 2018;12(2):217–229. doi:10.1093/ecco-jcc/jjx115
48. Gao S, Tian B, Han J, et al. Enhanced transdermal delivery of lornoxicam by nanostructured lipid carrier gels modified with poly-arginine peptide for treatment of carrageenan-induced rat paw edema. *Int J Nanomedicine*. 2019;14:6135–6150. doi:10.2147/IJN.S205295
49. Du Q, Chen J, Yan G, et al. Comparison of different aliphatic acid grafted N-trimethyl chitosan surface-modified nanostructured lipid carriers for improved oral kaempferol delivery. *Int J Pharm*. 2019;568:118506. doi:10.1016/j.ijpharm.2019.118506
50. Serafim TL, Oliveira PJ, Sardao VA, Perkins E, Parke D, Holy J. Different concentrations of berberine result in distinct cellular localization patterns and cell cycle effects in a melanoma cell line. *Cancer Chemother Pharmacol*. 2008;61(6):1007–1018. doi:10.1007/s00280-007-0558-9
51. Yin J, Hou Y, Yin Y, Song X. Selenium-coated nanostructured lipid carriers used for oral delivery of berberine to accomplish a synergic hypoglycemic effect. *Int J Nanomedicine*. 2017;12:8671–8680. doi:10.2147/ijn.s144615
52. Takashima T, Sakata Y, Iwakiri R, et al. Feeding with olive oil attenuates inflammation in dextran sulfate sodium-induced colitis in rat. *J Nutr Biochem*. 2014;25(2):186–192. doi:10.1016/j.jnutbio.2013.10.005
53. Wullaert A, Bonnet MC, Pasparakis M. NF-κB in the regulation of epithelial homeostasis and inflammation. *Cell Res*. 2011;21(1):146–158. doi:10.1111/imr.12550
54. Owczarek K, Koziołkiewicz M, Hrabec E, et al. Flavanols from Japanese quince (Chaenomeles japonica) fruit suppress expression of cyclooxygenase-2, metalloproteinase-9, and nuclear factor-kappaB in human colon cancer cells. *Acta Biochim Pol*. 2017;64(3):567–576. doi:10.18388/abp.2017_1599
55. Ain Q, Schmeer C, Penndorf D, et al. Cell cycle-dependent and -independent telomere shortening accompanies murine brain aging. *Aging*. 2018;10(11):3397–3420. doi:10.18632/aging.101655
56. Xiang H, Lin L, Hu X, et al. AMPK activation attenuates inflammatory pain through inhibiting NF-κB activation and IL-1β expression. *J Neuroinflammation*. 2019;16:34. doi:10.1186/s12974-019-1411-x